Solid State Sciences 106 (2020) 106297

Contents lists available at ScienceDirect

Solid State Sciences

journal homepage: http://www.elsevier.com/locate/ssscie

Temperature dependent I–V characterization of Coronene/p-Si based heterojunctions: Space charge limited current, Schottky emission at high voltages, thermionic emission and pool-Frenkel emission at low voltages

M.M. El-Nahass, H.A.M. Ali *

Physics Department, Faculty of Education, Ain Shams University, Roxy, 11757, Cairo, Egypt

ARTICLE INFO

Handling Editor: Mme B. Albert

Keywords:
Coronene thin film
Organic/inorganic heterojunction
Photovoltaic characteristics

ABSTRACT

A Heterojunction of Au/Coronene/p-Si/Al was fabricated by thermal evaporation technique. The features of current-voltage (I–V) were examined under dark condition at several temperatures in 292–373 K range. Extensive analysis of I–V curves in forward bias demonstrated that the mechanisms of thermionic emission and space charge limited currents represent the dominant mechanisms in the low and high range of used voltages, respectively. The reverse I–V curves were interpreted via Poole– Frenkel and Schottky effects. Some specific parameters were estimated as diode ideality factor, series resistance and shunt resistance. The photovoltaic manner of Coronene/p-Si heterojunction was shown under illumination. The cell parameters were evaluated from the analysis; open circuit voltage, short circuit current and fill factor.

1. Introduction

Organic conjugated materials offer remarkable attention as key building blocks of many electronic devices and molecular electronics [1–3] because of their simplicity of processability and chemical tunability causes them predestined for uses in effective and low-priced broad area of electronics [1]. They are interesting because of their potentially large optical response properties. Besides the existences of strong intermolecular charge transfer excitations in a molecular environment makes them important to nonlinear optical activity behavior [4]. Also, these materials have prosperous electrical, optoelectronic, and storage properties for electronic device development and manufacturing [5]. Many studies have been reported on these properties. Saran et al. [6] fabricated One dimensional single-crystal nanorods of C_{60} as a flexible photoconductor and it showed unique optoelectronic properties including high electron mobility, high photosensitivity and an excellent electron accepting nature. Li et al. [7] presented studies on the high-mobility field-effect Transistors from large-area solution grown aligned C_{60} single crystals.

Furthermore, Polycyclic aromatic hydrocarbons, PAHs, are broadly utilized as dynamic components in assorted opto-electronic devices, in their crystalline and thin-film forms [8]. They are widely researched molecules, as they exhibit a rigid planar structure, high stabilities and characteristic optical and electronic behavior [9]. Also, PAHs have an extended electron-rich π-system, which provides effective interaction with planar acceptor molecules and enhances the lateral ordering in the thin films, as well as close packing and order in single crystals [10]. Thus, PAHs give high performance as organic thin film in photovoltaic cells, field-effect transistors, light-emitting diodes and liquid crystals [8]. Coronene molecule is one PAHs with molecular structure displayed in Fig. 1. It is made out of six aromatic rings organized in a planar discoidal geometry. It exhibits molecular symmetry (D6h), 24 electron p-system [11,12]. Its shape of disk-like provides additional degree of freedom of coronene in crystalline materials and allows its rotation around the axis perpendicular to the molecular plane [13]. Akın et al. [14] investigated optoelectronic properties of the prepared Coronene thin films/n-Si by spin coating method as based photodiodes. It showed a photovoltaic status with a maximum short-circuit current of 13.1 μA and open circuit voltage of 0.16 V under 100 mW/cm^2 illumination intensity and the recombination processes presented the existence of bimolecular recombination mechanism associated with the trap levels in the band gap. Barış et al. [15] fabricated coronene nanowires by means of physical vapor deposition and reported on the optical energy gap of coronene nanowires that was found as 3.5 eV from the optical absorption in the wavelength range 200–2500 nm.

Studies on Current-Voltage (I–V) characteristic estimations are

* Corresponding author.
E-mail address: hend2061@yahoo.com (H.A.M. Ali).

https://doi.org/10.1016/j.solidstatesciences.2020.106297
Received 22 February 2020; Received in revised form 16 May 2020; Accepted 22 May 2020
Available online 28 May 2020
1293-2558/© 2020 Elsevier Masson SAS. All rights reserved.

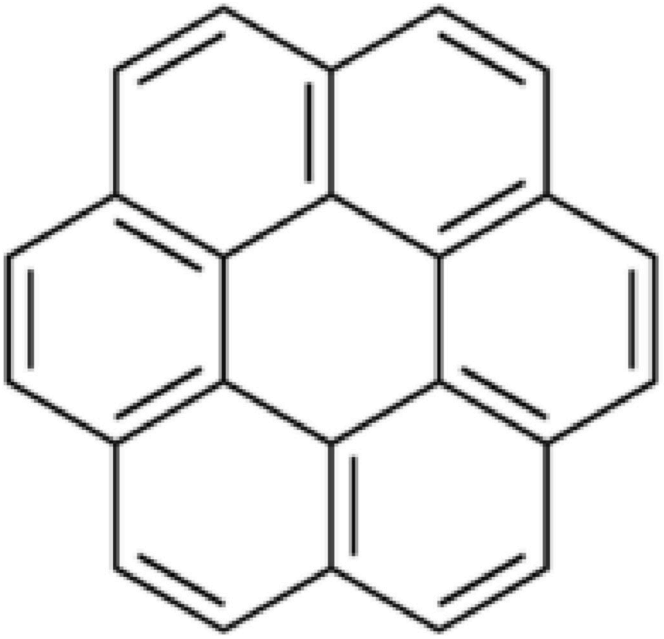

Fig. 1. Molecular structural of coronene.

utilized for the assessment of the performances of conventional organic photovoltaic cells. The analysis of the current-voltage curves gives a lot of information about the properties of the conducting materials when used in many other applications [16]. The present paper is dedicated to the electrical characterization of Coronene/p-Si heterojunction fabricated by thermal evaporation. The characteristics of current – voltage (I–V) and their fundamental parameters were examined under temperature varied from 292 to 373 K. The mechanisms for current transport for both forward and reverse bias were detected. The photovoltaic behavior of heterojunction Coronene/p-Si was investigated under illumination of light.

2. Experimental details

Heterojunction cell of Coronene/p-Si was fabricated by thermal evaporation of Coronene onto p-type (100) silicon single-crystal, doped with 10^{16} cm^{-3}, as a substrate. A high vacuum coating unit (type E306A, Edwards Co., England) was utilized for the fabrication process of deposition rate 2.5 nm/s and under a vacuum of 10^{-4} Pa. The p-silicon wafer was etched as mentioned elsewhere [17], where the surface of a silicon wafer was treated with a buffer etchant of CP4 solution (HF: HNO_3:CH_3COOH in the ratio1:6:1) for 8s, that removed effectively the surface film of silicon dioxide. Then, the Si wafer was washed for 2 min in pure alcohol and distilled water to utilize it as a substrate for heterojunction fabrication. The substrate temperature was kept at room temperature during the deposition procedure. Aluminum was deposited onto Si as a back electrode. The other side of p-Si was covered by depositing a thin film of coronene with 100 nm thickness. The front contact was made with gold mesh electrode. The heterojunction cell of Au/Coronene/p-Si/Al was obtained. A high impedance programmable electrometer (Keithley 2635A) was used to record the current–voltage (I–V) measurements of Coronene/p-Si heterojunction under dark condition for various temperatures ranged from 292 to 373 K. Also, the Coronene/p-Si cells were exposed to light coming from a white light source (tungsten lamp) with intensity of 40 mW/cm^2 at room temperature to determine the photovoltaic behavior of Coronene/p-Si cell under illumination.

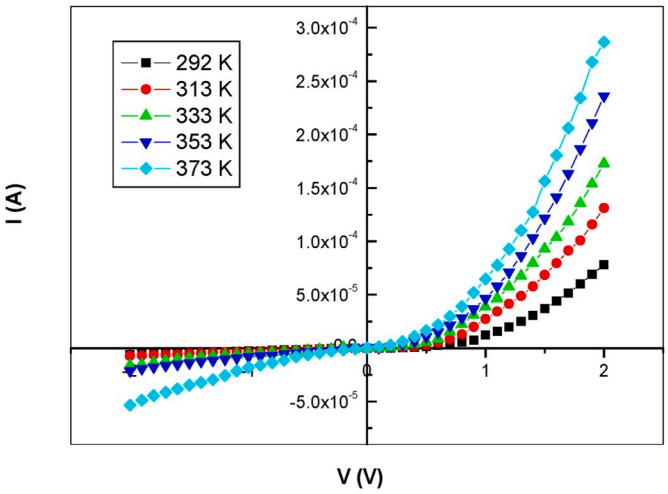

Fig. 2. I–V characteristics of Au/coronene/p-Si heterojunction at different temperatures.

Table 1
I–V characteristics parameters for Coronene/p-Si heterojunction.

T(K)	292	313	333	353	373
R.R	9.03	13.42	10.12	8.78	4.51
R_s (kΩ)	26.04	15.39	11.58	8.54	7.02
R_{sh} (MΩ)	2.59	1.24	0.51	0.20	0.09
I_o (mA)	1.54 × 10^{-5}	3.25 × 10^{-5}	6.00 × 10^{-5}	1.32 × 10^{-4}	2.46 × 10^{-4}

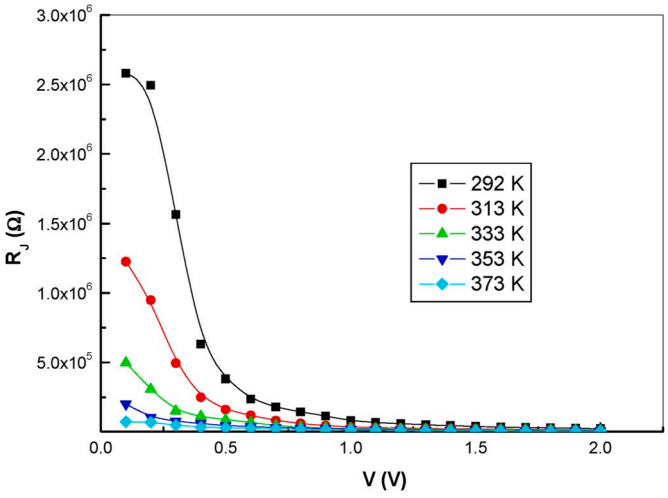

Fig. 3. Plot of R_j versus voltage for Au/coronene/p-Si heterojunction at different temperatures.

3. Results and discussion

The current-voltage (I–V) characteristics of Coronene/p-Si heterojunction in the dark at different temperature is represented in Fig. 2. The trend of curves of I–V represents a diode like behavior, where the current of Coronene/p-Si heterojunction increases with the increase in voltage in forward and reverse bias from 2 V to −2 V. This is a sufficient indication for the formation of a depletion region between Coronene and Si that limits the forward and reverse carrier flowing across the junction [18]. The rectification ratio, RR, Coronene/p-Si heterojunction is recorded as the ratio of the forward current to reverse current at a

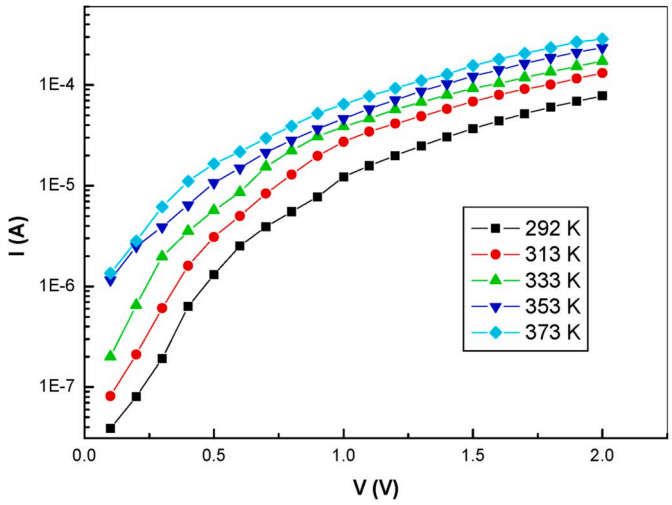

Fig. 4. The forward semi-logarithmic I–V characteristics of Au/coronene/p-Si heterojunction at different temperatures.

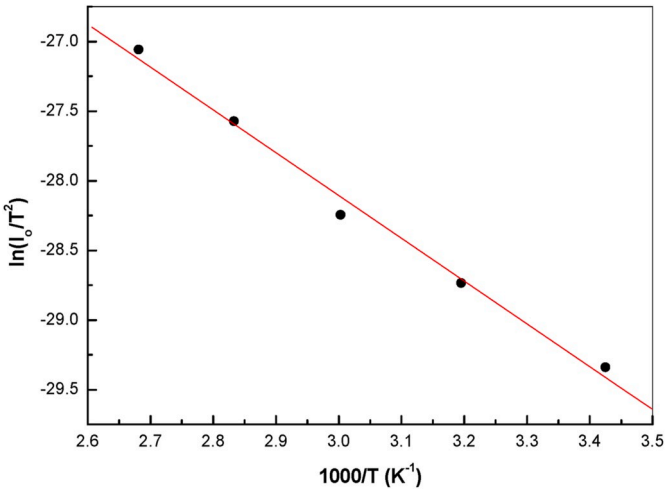

Fig. 5. Plots of the ln (I_o/T^2) versus 1000/T of Au/coronene/p-Si heterojunction.

certain applied voltage. The RR values were recorded at different temperatures at ±1.5 V as found in Table 1. The trend of R.R showed a decrease with rising temperature which might be due to the raising leakage current with raising temperature of the heterojunction [19].

The series resistance, R_s, and shunt resistance, R_{sh}, are crucial parameters for solar cells and heterojunctions that impact the achievement of these devices. The R_s is active at adequate high forward biases and R_{sh} is active in the reverse bias region or close to zero bias. R_s and R_{sh} Coronene/p-Si heterojunction are determined for the I–V data, where the junction resistance is $R_j = \partial V_j/\partial I_j$ [20] as seen in Fig. 3. At higher forward bias, the value of R_j becomes nearly constant for each temperature and indicates to R_s. At zero bias, the value of R_j reaches its maximum points to the values of R_{sh}. Table 1 shows the values of R_s and R_{sh} for Coronene/p-Si heterojunction at different temperatures.

Fig. 4 offers a semi-logarithmic plot of the forward I–V curves of Coronene/p-Si heterojunction for various temperatures. The I–V curves can be arranged into two distinct regions as indicated by the applied voltages range, where at voltages higher than 0.7 V the curves deviated from the linearity attributable to the impact of series resistance R_s [21,22]. The forward I–V characteristics at low voltage range ˂ 0.7 V can expressed by the equations of the model of thermionic emission [23]:

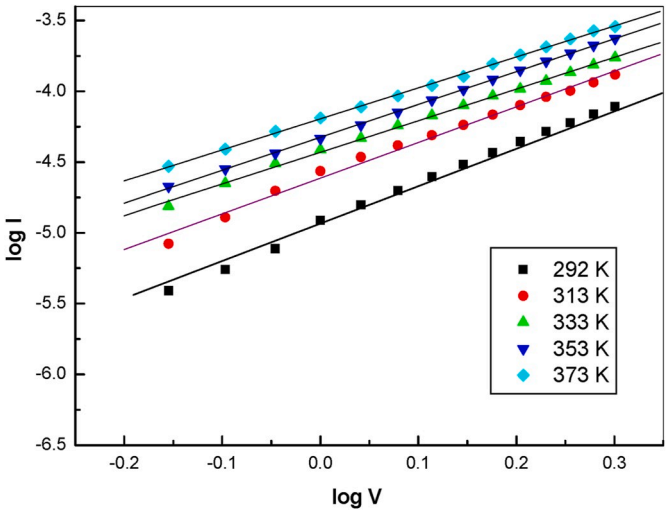

Fig. 6. Plot of log I versus log V of Au/coronene/p-Si heterojunction at high voltage for different temperatures.

$$I = I_o\left[e^{q(V-IR_s)/mkT} - 1\right] \quad (1)$$

And the reverse saturation current is given as:

$$I_o = AA^*T^2e^{\left(-\frac{q\phi}{kT}\right)} \quad (2)$$

where m represents the diode ideality factor, A* is the effective Richardson constant. A is the effective area of the diode and T is the absolute temperature. ϕ is the barrier height that exists at the interface between the organic and the inorganic layers [24]. The values of I_o of Coronene/p-Si are tabulated in Table 1 for different temperatures. To assign ϕ value, a plot of ln (I_o/T^2) against 1000/T is presented in Fig. 5 and using the slope of the obtained straight line, the barrier height is evaluated as 0.26 eV. At this low voltage region, the diode ideality factor for Coronene/p-Si heterojunction specified as [25]:

$$m = \frac{q}{kT}\frac{dV}{d(\ln I)} \quad (3)$$

The ideality factor supplies valuable data upon the transport and recombination processes in organic solar cells [26]. The recorded diode ideality factor for Coronene/p-Si heterojunction at this range of voltages

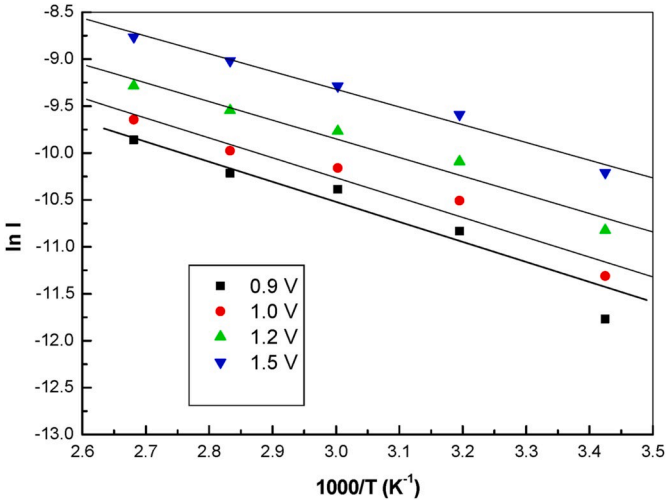

Fig. 7. Plot of ln I versus 1000/T of Au/coronene/p-Si heterojunction at a fixed voltage.

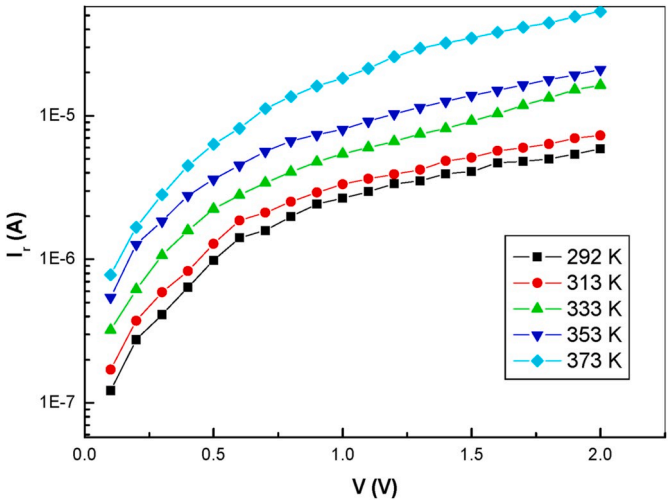

Fig. 8. The reverse semi-logarithmic I–V characteristics of Au/coronene/p-Si heterojunction.

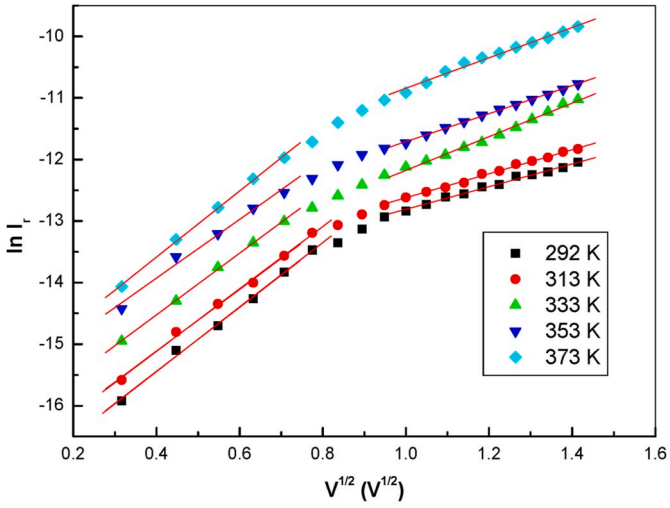

Fig. 9. Plot of ln I_r versus $V^{1/2}$ of Au/coronene/p-Si heterojunction at different temperatures.

found as 3.99 ± 0.16 for the inspected temperature range. Increasing ideality factor above unity probably refers to non-homogeneity of film thickness, interface states and non-uniformity distribution of the interfacial charges [27].

In the higher voltage region, V ˃ 0.7 V, the current points to a power dependence of voltage I α V^u with a slope (u) of ~2 for the plot of log-I–logV as shown in Fig. 6. This power reliance reveals that current transport is consistent with space-charge-limited current density (SCLC) dominated by a single trap level mechanism in Coronene/p-Si. The forward current in this mechanism is expressed as [28]:

$$I = \frac{9}{8}\varepsilon\mu\left(\frac{N_c}{N_t}\right)\left(\frac{V^2}{d^3}\right)e^{\left(\frac{-E_t}{kT}\right)} \quad (4)$$

where N_c is the density of states in the valence band, N_t is the concentration of traps at energy level E_t, over the valence band edge, and d is the Coronene thin film. Fig. 7 represents the plot of ln(I) versus 1000/T in SCLC region at a fixed bias potential (0.9, 1, 1.2 and 1.5 V). The estimation of E_t is determined from the slope of straight-line fitting inFig. 7 and is found as 0.17 eV.

Information about the properties of metal-semiconductor contact can

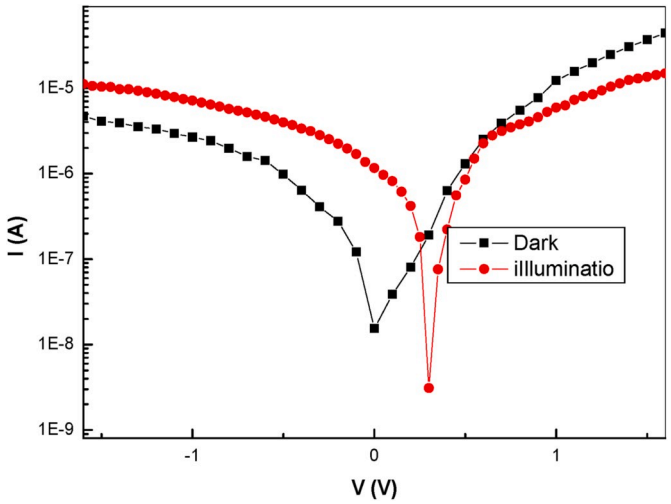

Fig. 10. Semi-logarithmic I–V characteristics of Au/coronene/p-Si heterojunction under dark and illumination condition.

be expressed by the behavior of I–V characteristics in reverse bias [29]. The reverse I–V curves of Coronene/p-Si heterojunction are displayed in Fig. 8 at different temperatures. As seen, the reverse bias current increases as the temperatures raises. Fig. 9 shows the plot of reverse current (lnI_r) versus $V^{1/2}$ for different temperatures. It is seen from the figure that these curves show a linear dependence in two segments with different slope values and consequently the reverse current might be clarified in terms of two different mechanisms. These mechanism for current can be referred to Poole-Frenkel emission or Richardson Schottky emission mechanisms [29–32].

In Poole-Frenkel emission, the current is given by:

$$I_r = I_{PF}\ e^{\left(\beta_{PF}V^{1/2}/kTd^{1/2}\right)} \quad (5)$$

In Richardson Schottky emission, the current is given by:

$$I_r = AA^*T^2e^{(-\phi_s/kT)}e^{\left(\beta_sV^{1/2}/kTd^{1/2}\right)} \quad (6)$$

where ϕ_s is the Schottky-barrier height at the injected electrode interface, I_{PF} is the low-field current density and β_{PF} and β_s are the Poole-Frenkel and Schottky field lowering coefficients, respectively, which are linked by:

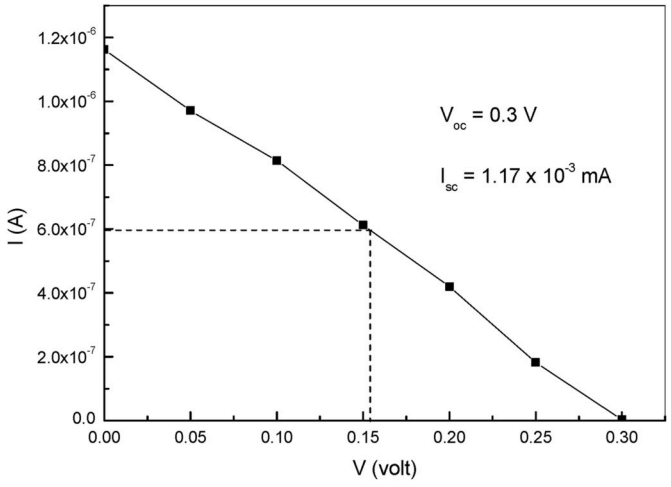

Fig. 11. I–V characteristics under illumination of Au/coronene/p-Si heterojunction.

$$\beta_{PF} = 2\beta_s \sqrt{\frac{q^3}{\pi \varepsilon_o \varepsilon_r}} \quad (7)$$

where ε_o represents the permittivity of free space and ε_r represents the relative permittivity of the material (for coronene $\varepsilon_r = 3$ [33]). The calculated theoretical values for β_{PF} and β_s are 4.46×10^{-5} and 2.23×10^{-5} $eVm^{1/2} V^{-1/2}$, respectively. Using the slope of the linear segment in Fig. 9, the average β experimental value (4.73×10^{-5}) in the first segment of voltage ˂ 0.7 V is closely related to the theoretical value of β_{PF}. This suggests that Poole-Frenkel emission is dominant for current transport at lower applied voltages. While in the second segment of voltage ˃ 0.7 V, β experimental value (1.74×10^{-5}) $eVm^{1/2} V^{-1/2}$ is closely related to the theoretical value of β_s. This is an indication to the Richardson Schottky emission, that is the dominant mechanism in this range of voltages.

The photovoltaic properties of the Coronene/p-Si device are determined by measuring the I–V/cm^2 characteristics under illumination of power density 40 mW/cm^2. Fig. 10 shows the I–V behavior under dark and illumination conditions. The illumination current observed to be large at the negative bias. This points out that the light illumination increases production of electron–hole pairs [34]. This suggests that the Coronene/p-Si heterojunction owns a photovoltaic behavior. Fig. 11 represent photovoltaic behavior of Coronene/p-Si device under illumination. The device parameters for Coronene/p-Si; open circuit voltage (V_{oc}) and short circuit current (I_{sc}) are found to be 0.3 V and 1.17×10^{-3} mA, respectively. The fill factor (FF) of a photovoltaic Coronene/p-Si device can be expressed as [35]:

$$FF = \frac{V_m I_m}{V_{oc} I_{sc}} \quad (8)$$

where V_m and I_m are the values for which the maximum electrical power can be extracted from a solar cell. The estimated FF is about 0.26. The low value of FF can be referred to mechanisms of the charge photogeneration process or large series resistance of the organic layer [36].

4. Summary

The Au/Coronene/p-Si/Al heterojunction was fabricated by thermal evaporation technique. The curves of I–V showed diode like behavior. The trend of R.R showed a decrease with the rise in temperature. The values of R_s and R_{sh} for Coronene/p-Si heterojunction decreased as the temperature increase from 292 to 373 K. The forward bias current was explicated with two different mechanisms; thermionic emission with barrier height of 0.26 eV and diode ideality factor of about 3.99 ± 0.16 deduced in the examined range of temperature at low forward bias. The space-charge limited currents with a single trap level deduced at high forward bias where the current points to a power dependence of voltage $I \alpha V^u$ with a slope (u) of ~2. The trap level energy was at 0.17 eV. The Poole-Frenkel emission was the dominant mechanism at voltage ˂ 0.7 V for the reverse current. The Schottky emission was the dominant mechanism at higher voltages. The estimated parameters of Coronene/p-Si device were open circuit voltage, short circuit current and Fill factor and found to be 0.3 V, 1.17×10^{-3} mA and 0.26, respectively.

In Conclusion, For Coronene/p-Si heterojunction, the current transport under the forward bias was controlled by thermionic emission and SCLC mechanisms at low and high voltages, respectively. Under the reverse bias; By comparing the experimental values of the β_{PF} and β_s coefficient with the theoretical ones, the Poole-Frenkel emission was the dominant mechanism at low voltages and the Schottky emission was at high voltages for the current transport.

Ethical statement

The article is the original one and it did not send to other journals. The co-authors of this paper agree to publish it in this journal.

Declaration of competing interest

The authors declare that they have no known competing financial interests or personal relationships that could have appeared to influence the work reported in this paper.

References

[1] T. Storzer, A. Hinderhofer, C. Zeiser, J. Nov'ak, Z. Fiser, V. Belova, B. Reisz, S. Maiti, G. Duva, R.K. Hallani, A. Gerlach, J.E. Anthony, F. Schreiber, J. Phys. Chem. C 121 (38) (2017) 21011.
[2] J.L. Bre ˈdas, J.P. Calbert, D.A. da Silva Filho, J. Cornil, Proc. Natl. Acad. Sci. Unit. States Am. 99 (2002) 5804.
[3] M.M. El-Nahass, H. Abdel-Khalek, E. Salem, Am. J. Mater. Sci. 2 (4) (2012) 131.
[4] G.W. Ejuh, F. Tchangnwa Nya, M.T. Ottou Abe, F.F. Jean-Baptiste, J.M.B. Ndjaka, Opt. Quant. Electron. 49 (2017) 382.
[5] E.F.M. El-Zaidia, H.A.M. Ali, Taymour A. Hamdalla, A.A.A. Darwish, T.A. Hanafy, Opt. Mater. 100 (2020) 109661.
[6] R. Saran, V. Stolojan, R.J. Curry, Sci. Rep. 4 (2014) 5041.
[7] H. Li, B.C.-K. Tee, J.J. Cha, Y. Cui, J.W. Chung, S.Y. Lee, Z. Bao, J. Am. Chem. Soc. 134 (2012) 2760.
[8] P. Mocci, R. Cardia, G. Cappellini, J. Phys.: Conf. Series 956 (2018), 012020.
[9] J. Potticary, L.R. Terry, C. Bell, A.N. Papanikolopoulos, P.C.M. Christianen, H. Engelkamp, A.M. Collins, C. Fontanesi, G. Kociok-Köhn, S. Crampin, E. Da Como, S.R. Hall, Nat. Commun. 7 (2016) 11555.
[10] O. Kataeva, M. Khrizanforov, Y. Budnikova, D. Islamov, T. Burganov, A. Vandyukov, K. Lyssenko, B. Mahns, M. Nohr, S. Hampel, M. Knupfer, Cryst. Growth Des. 16 (2016) 331.
[11] A. Soncini, E. Steiner, P.W. Fowler, R.W.A. Havenith, L.W. Jenneskens, Chem. Eur J. 9 (2003) 2974.
[12] Y. Zhao, D. Truhlar, J. Phys. Chem. C 112 (2008) 4061.
[13] T. Heinemann, K. Palczynski, J. Dzubiella, S.H.L. Klapp, J. Chem. Phys. 141 (2014) 214110.
[14] Ü. Akın, Ö.F. Yüksel E. Taşcı, N. Tuğluoğlu, Siliconindia (2019), https://doi.org/10.1007/s12633-019-00233-2.
[15] B. Barış, S. Karadeniz, M. Okan Erdal, Mater. Lett. 205 (2017) 70.
[16] C. Zhang, J. Zhang, Y. Hao, Z. Lin, C. Zhu, J. Appl. Phys. 110 (6) (2011), 064504.
[17] A.A.A. Darwish, T.A. Hanafy, A.A. Attia, D.M. Habashy, M.Y. El-Bakry, M.M. El-Nahass, Superlattice. Microst. 83 (2015) 299.
[18] A. Attia, H.A.M. Ali, G.F. Salem, M.I. Ismail, F.F. Al-Harbi, Opt. Mater. 66 (2017) 480.
[19] H.M. Zeyada, M.M. El-Nahass, E.M. El-Menyawy, A.S. El-Sawa, Synth. Met. 207 (2015) 46.
[20] S. Alialy, S. Altındal, E.E. Tanrıkulu, D.E. Yıldız, J. Appl. Phys. 116 (2014), 083709.
[21] M.M. El-Nahass, A.M. Farid, A.A.M. Farag, H.A.M. Ali, Vacuum 81 (2006) 8.
[22] A. Ashery, H.S. Metwally, F.S. Terra, A.A. El-Shazly, Ind. J. pure Appl. Phys 39 (2001) 450.
[23] S.H. Kim, C.Y. Jung, H. Kim, Y. Cho, D.-W. Kim, Transactions on electrical and electron, Materials 16 (2015) 151.
[24] A.A. Hendi, E.F.M. El-Zaidia, Synth. Met. 199 (2015) 388.
[25] Z. Khurelbaatar, K.-H. Shim, J. Cho, H. Hong, V.R. Reddy, C.-J. Choi, Mater. Trans. 56 (1) (2015) 10.
[26] G.A.H. Wetzelaer, M. Kuik, M. Lenes, P.W.M. Blom, Appl. Phys. Lett. 99 (2011) 153506.
[27] V. Lakshmi Devi, I. Jyothi, V. Rajagopal Reddy, Chel-Jong Choi, Open Appl. Phys. J. 5 (2012) 1.
[28] R.D. Gould, J. Appl. Phys. 53 (1982) 3353.
[29] G.D. Sharma, Synth. Met. 74 (1995) 227.
[30] H.A.M. Ali, H.S. Soliman, KhM. Eid, S.M. Atef, Mater. Chem. Phys. 142 (2013) 132.
[31] S.B.K. Aydin, D.E. Yildiz, H.K. Çavus, R. Sahingoz, Bull. Mater. Sci. 37 (7) (2014) 1563.
[32] H.M. Chenari, H. Sedghi, M. Talebian, Mir M. Golzan, A. Hassanzadeh, J. Nanomater. 1 (2011). Article ID 190391.
[33] J. Swiatek, Phys. Status Solidi a (88) (1976) 285.
[34] C. Ozaydin1, K. Akkilic, Am. J. Optic. Photon. 2 (6) (2014) 69.
[35] B.P. Rand, J. Genoe, P. Heremans, J. Poortmans, J. Poortmans, Prog. Photovoltaics Res. Appl. 15 (2007) 659.
[36] A.A.A. Darwish, E.A.A. El-Shazly, A.A. Attia, K.F. Abd El-Rahman, J. Mater. Sci. Mater. Electron. 27 (2016) 8786.